ELSEVIER

Throughput-coverage tradeoff in a scalable wireless mesh network ☆

Jane-Hwa Huang*, Li-Chun Wang, Chung-Ju Chang

Department of Communication Engineering, National Chiao Tung University, Taiwan, ROC

Abstract

The wireless mesh network (WMN) is an economical and low-power solution to support ubiquitous broadband services. However, mesh networks face scalability and throughput bottleneck issues as the coverage and the number of users increase. Specifically, if the coverage is extended by multiple hops, the repeatedly relayed traffic will exhaust the radio resource and degrade user throughput. Meanwhile, as the traffic increases because of more users, the throughput bottleneck will occur at the users close to the gateway. The contention collisions among these busy users near the gateway will further reduce user throughput. In this paper, a newly proposed scalable multi-channel ring-based WMN is employed. Under the ring-based cell structure, multi-channel frequency planning is used to reduce the number of contending users at each hop and overcome the throughput bottleneck issue, thereby making the system more scalable to accommodate more users and facilitate coverage extension. This paper mainly focuses on investigating the overall tradeoffs between user throughput and cell coverage in the ring-based WMN. An analytical throughput model is developed for the ring-based WMN using the carrier sense multiple access (CSMA) medium access control (MAC) protocol. In the analysis, we also develop a bulk-arrival semi-Markov queueing model to describe user behavior in a non-saturation condition. On top of the developed analytical model, a mixed-integer nonlinear optimization problem is formulated, aiming to maximize cell coverage and capacity. Applying this optimization approach, we can obtain the optimal number of rings and the associated ring widths of the ring-based WMN.
© 2007 Elsevier Inc. All rights reserved.

1. Introduction

With the abilities of enhancing coverage and capacity by low transmission power, wireless mesh networks (WMNs) play a significant role in providing ubiquitous broadband access [1,7,18,21,22,25]. Fig. 1 shows a multi-hop WMN, where each user relays other users' traffic toward the central gateway and only the gateway directly connects to the Internet. In general, the advantages of WMN can be summarized into four folds. First, WMN can combat shadowing and path loss to extend

service coverage. Second, WMN can be rapidly deployed in a large-scale area with less cabling engineering work and infrastructure costs [7,18,21,25]. Third, WMN can concurrently support various wireless radio and access technologies such as 802.16 (WiMAX), 802.11 (WiFi), and 802.15 (Bluetooth and Zigbee), thereby providing the flexibility to integrate different radio access networks [1]. Fourth, WMN can be managed in a self-organization and self-recovery fashion [1,22]. If some nodes malfunction, the traffic can be forwarded by alternative nodes.

However, WMNs face scalability issue because throughput enhancement and coverage extension are usually two contradictory goals in WMNs [1,11,17,18,21]. Specifically, the multi-hop communications can extend the coverage of gateway to serve more users by more hops and longer hop distance. However, the repeatedly relayed traffic with more hops will exhaust the radio resource and thus degrade the user throughput [11,17]. The longer hop distance will lower the data rate in the relay link between users. Moreover, increasing traffic from

* Corresponding author. Fax: +886 3 571 0116.
E-mail addresses: hjh@mail.nctu.edu.tw (J.-H. Huang), lichun@cc.nctu.edu.tw (L.-C. Wang), cjchang@cc.nctu.edu.tw (C.-J. Chang).
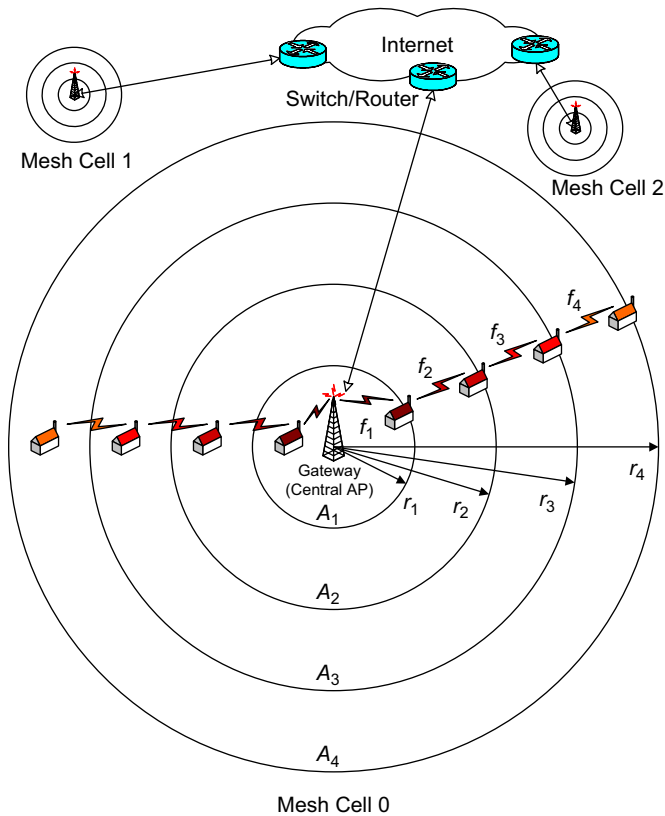
Fig. 1. Ring-based cell architecture for a scalable wireless mesh network, where each ring is allocated with different channels.

more users will induce the throughput bottleneck at the users near the gateway, thereby further degrading user throughput. Therefore, while multi-hop communication is used to extend coverage with more users, how to improve user throughput is a key challenge in designing a scalable WMN.

In the literature, the performances of WMNs have been studied mainly from two directions [9,18–21]. On one hand, the authors in [20] demonstrated the advantage of a multi-hop WMN over a single-hop network in terms of coverage by simulations. On the other hand, the results in [9,19] showed that with k users in an ad hoc network, the throughput per user is scaled like $O(1/\sqrt{k \log k})$. Moreover, the authors in [18] pointed out that the user's throughput in the WMN decreases sharply as $O(1/k)$ because of the throughput bottleneck at the gateway. To resolve the scalability issue, our previous work [13] proposed a ring-based WMN. The work in [13] investigated the delay and cell capacity tradeoff in a WMN. To our knowledge, a few papers have studied the overall performances of user throughput and cell coverage of the WMN [21]. However, the work [21] considered the single-user case.

To resolve the scalability and throughput bottleneck issues, this paper employs the newly proposed ring-based WMN in [13], where the rings in a cell are allocated with different channels as shown in Fig. 1. This WMN is scalable due to the following two factors. First, multi-channel frequency planning can reduce the number of users contending for the same channel, and overcome the throughput bottleneck issue at the gateway.

Second, with the capability to adjust the ring width to control the contention level, the ring structure can facilitate managing throughput in a WMN.

This paper investigates the optimal tradeoff between user throughput and cell coverage in the scalable ring-based WMN. We develop an analytical throughput model by considering the impacts of ring-based cell structure and frame contentions in the carrier sense multiple access (CSMA) medium access control (MAC) protocol. In the throughput analysis, we also develop a bulk-arrival semi-Markov model to describe user behavior under the non-saturation condition. On top of the developed analytical model, we formulate an optimization problem aiming to improve the performance tradeoff between throughput and coverage. With the optimization technique, we can determine the optimal number of rings and the associated ring widths in a mesh cell.

The rest of this paper is organized as follows. Section 2 discusses the considered scalable ring-based WMN. In Section 3, we formulate an optimization problem to maximize coverage and capacity of a mesh network. Section 4 investigates the channel activity in the ring-based WMN, with considering the impact of ring structure on frame contentions. On top of the channel activity concept, in Section 5 we develop a MAC throughput model for the considered WMN. Numerical examples are shown in Section 6. Concluding remarks are given in Section 7.

2. Scalable ring-based WMN

2.1. Network architecture and assumptions

Fig. 1 shows the scalable ring-based WMN, where stationary mesh users form a multi-hop network to extend cell coverage. The mesh cell is divided into several rings A_i, $i = 1, 2, \ldots, n$, determined by n concentric circles centered at the gateway with radii $r_1 < r_2 < \cdots < r_n$. The user in ring A_i connects to the gateway by an i-hop communication. The users in the inner rings will relay data for users in the outer rings toward the gateway and only the gateway connects to the Internet directly. Clearly, this WMN can be rapidly deployed in a large-scale area with less cabling engineering work.

The ring-based WMN operates in a multi-channel with multi-interface fashion. In a mesh cell, the rings are allocated with different channels to avoid inter-ring co-channel interference and reduce contention collisions. As shown in Fig. 1, the user in ring A_i communicates with the users in rings A_{i-1} and A_{i+1} at different channels f_i and f_{i+1}, respectively. This frequency planning is simple because it only needs to design each ring width to ensure a sufficient co-channel reuse distance without interference. We also assume that each user is equipped with two radio interfaces as in [1]. With multiple interfaces independently operating at different channels, each user can concurrently receive and deliver the relay traffic, thereby improving the throughput and delay performances. In addition, the WMN can work well even if employing the legacy CSMA MAC protocol, which in turns avoids complexity and compatibility issues.
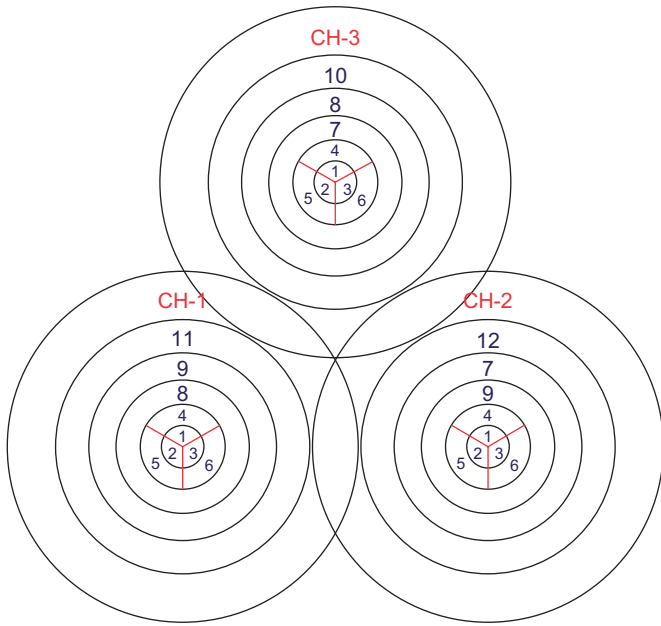
Fig. 2. Example of a three-cell WMN with 12 available channels. Four buffer rings between two co-channel rings are ensured, and the congested inner rings (A_1–A_2) are sectorized.

Spectrum and hardware costs are the major concerns in the multi-channel with multi-interface systems. However, there are multiple channels available in wireless local area networks (WLANs), for example, 12 channels assigned for the IEEE 802.11a WLAN [16,23]. The price of radio interface also goes down rapidly, since the WLAN has become an off-the-shelf product.

2.2. Ring-based frequency planning

Now, we explain the ring-based frequency assignment by a three-cell WMN as shown in Fig. 2. In this example, channels 1–3 and 4–6 are assigned to the sectors in the innermost rings A_1 and A_2 of each cell. Channels 7–9 are repeatedly allocated to the middle rings A_3 and A_4 of the cells with four buffer rings. Channels 10–12 are allocated to rings A_5 of the cells, respectively. Then, with four buffer rings, the channels 1–3 are reused in the outer rings A_6. This example shows that 12 available channels can ensure four buffer rings between two co-channel rings. Besides, the channels allocated to the inner rings can be spatially reused in the outer rings with a sufficient reuse distance.

Referring to Fig. 2, we also suggest sectorizing the congested inner rings and allocating a different channel to each sector, to overcome the throughput bottleneck issue near the gateway. In a WMN, the users in the inner rings near the gateway will relay more traffic than the users in the outer rings. By partitioning the inner rings into several sectors to reduce the number of contending users, the throughput can be further improved. In this example, the innermost rings of each cell are divided into three sectors. Apparently, if more non-overlapping channels are available, more inner rings can be sectorized without

inter-ring co-channel interferences to enhance cell capacity and coverage.

In practice, the WLAN users may interfere with this ring-based WMN operating at the unlicensed band, and thus the throughput of each user will decrease. In this situation, we suggest allocating the channels with less interference to the congested inner rings to ensure throughput. To understand performance bound of this multi-hop network, this interference issue is not considered in this paper.

2.3. Scalability

Most traditional WMNs are not scalable to cell coverage because the user throughput is not guaranteed with increasing collisions. By contrast, the employed ring-based WMN is scalable to coverage since the ring-based frequency planning can reduce the number of contending users to resolve the contention issue. Then, the user throughput can be ensured by properly designing the ring widths in a mesh cell. The remaining important problem lies in the way to determine the optimal ring widths to achieve the optimal performance tradeoff between user throughput and cell coverage.

3. Coverage and capacity maximization

3.1. Problem formulation

Both user throughput and cell coverage performance issues will impact the design of WMN. From a deployment cost perspective, a larger coverage per cell is better since fewer gateways are needed. From a user throughput viewpoint, however, a smaller cell is preferred since fewer users contend for the same channel. In the following, we formulate an optimization problem to find out the best number of rings and the optimal ring widths in a cell subject to the tradeoff between user throughput and cell coverage.

To begin with, we discuss the constraints in the considered optimization problem:

- The capacity $H_C(i)$ of the lowest-rate link in ring A_i should be greater than the carried traffic load R_i of one mesh user. That is,

$$H_C(i) = H_i(r_i - r_{i-1}) \geqslant R_i, \qquad (1)$$

where $(r_i - r_{i-1})$ is the width of ring A_i and $H_i(d)$ represents the link capacity between two users at a separation distance d. This constraint guarantees the minimum throughput for each user. Fig. 3 shows some examples of lowest-rate links, for example, the link between users $P_{C,i}$ and $Q_{C,i}$ at the ring boundaries with a separation distance $d = (r_i - r_{i-1})$.

- The ring width $(r_i - r_{i-1})$ should be less than the maximum reception range. Therefore,

$$(r_i - r_{i-1}) \leqslant d_{\max}. \qquad (2)$$

- The ring width should be greater than the average distance $d_{\min}$ between two neighboring users. Hence,
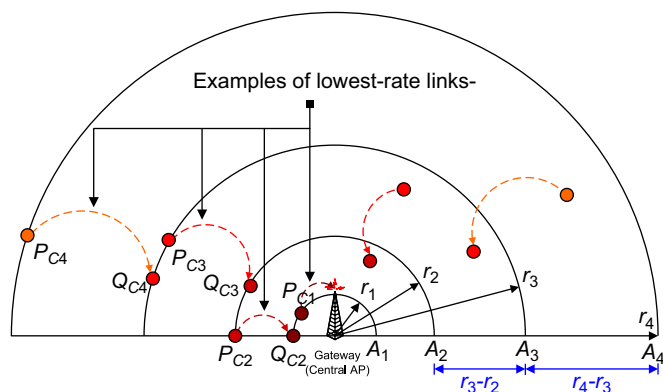
$$(r_i - r_{i-1}) \geqslant d_{\min}, \qquad (3)$$

Fig. 3. Examples of the lowest-rate links for a mesh cell with $n = 4$.

where $d_{\min} = 1/\sqrt{\rho}$ (m) is dependent on the user density ρ (users/m^2). This constraint also represents the limit on the hop distance due to user density.

3.2. Optimization approach

From the above considerations, the optimal cell coverage and capacity issues in a WMN can be formulated as a mixed-integer nonlinear programming (MINLP) problem with the nonlinear objective function (4). The decision variables includes the number of rings in a mesh cell, n (which is an integer) and the radii $r_1, r_2, \ldots, r_n$. The objective is to maximize the coverage of a mesh cell. In this scalable ring-based WMN, the ring-based frequency planning resolves the collision issue as cell overage increases. Therefore, the optimal coverage and capacity will be achieved simultaneously, since more users in a mesh cell can also lead to higher cell capacity. The optimal system parameters for the ring-based WMN can be determined by solving the following optimization problem:

$$\underset{n, r_1, r_2, \ldots, r_n}{\text{MAX}} \quad r_n \ (\text{cell coverage}), \tag{4}$$

$$\text{subject to} \quad H_C(i) \geqslant R_i, \tag{5}$$

$$d_{\max} \geqslant (r_i - r_{i-1}) \geqslant d_{\min}. \tag{6}$$

In this paper, cell coverage is defined as cell radius r_n, and cell capacity is the overall throughput of a cell, that is, $\rho \pi r_n^2 R_D$, where ρ is the user density, and R_D is the traffic load generated by each user.

4. Channel activity in the ring-based WMN

This section discusses the channel activity seen by an individual user employing the CSMA MAC protocol in the ring-based WMN. On top of the channel activity concept, we will develop an analytical throughput model for the considered WMN in Section 5.

From a particular user's viewpoint, there are five types of channel activities in the WMN:

(1) successful frame transmission;
(2) unsuccessful frame transmission;
(3) empty slot, where all users are in backoff or idle;
(4) successful frame transmission from other users;
(5) unsuccessful frame transmission from other users.

For clarity, the channel activity is described by a sequence of *activity time slots* [2,3,6]. Subject to the backoff procedures, the slot duration T_j for the channel activity type j is equal to

$$\begin{cases} T_1 = T_4 = T_S, \\ T_2 = T_5 = T_C, \\ T_3 = \sigma, \end{cases} \tag{7}$$

where σ is the duration of an empty slot, T_S and T_C are the successful transmission time and collision duration, respectively. Therefore, the average duration T_v of activity time slot can be written as

$$T_v = \sum_{j=1}^{5} v_j T_j. \tag{8}$$

Here, v_j is the corresponding probability for the channel activity type as calculated in the following, and $\sum_{j=1}^{5} v_j = 1$.

4.1. Assumptions

In the following, we consider the case where the traffic is unidirectional from the users to the gateway. The developed analytical method can be extended straightforwardly for the case with bidirectional traffic. We need to consider the contentions from the users with downlink traffic, and thus the number of contending users increases. It may also need to consider the asymmetric traffic load in downlink and uplink. Therefore, the users contending for the same channel may have different traffic loads. To clarify the developed analytical approach, this paper focuses on a simplified case with uplink traffic as an example.

To understand the coverage and capacity performance bounds in a ring-based WMN, we also assume that all the traffic is forwarded in the centripetal direction toward the gateway. Moreover, there always exists an intermediate relay node at the appropriate position. In a real WMN, the next-hop node may be too far away from the current node and therefore user throughput may degrade. In this situation, it may be needed to deploy a pure relay station to help forward data as discussed in [21]. In other cases, if the traffic is not forwarded in the centripetal direction, the throughput and coverage performances may degrade due to longer hop distance required.

4.2. Frame contention under ring-based cell structure

To investigate the channel activity in the ring-based WMN, we should consider the impacts of ring-based cell structure on frame contentions. At first, we define the *mutually interfered region* as an area in which any two users can sense the activity of each other. In Fig. 4, the area including users C and D is an example of a mutually interfered region. Since each ring
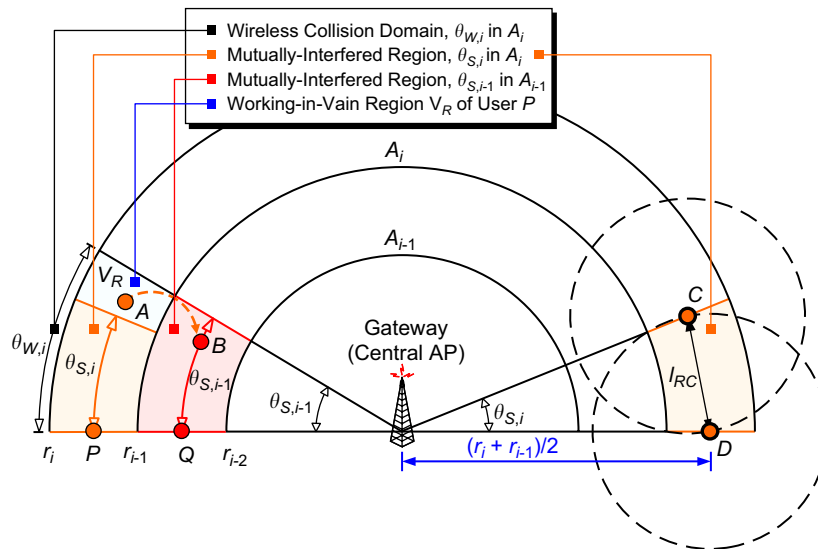
Fig. 4. Examples of wireless collision domain and mutually interfered region.

is allocated with a different channel, a mutually interfered region is the intersection of two circles and the associated ring, depending on the locations of considered users and the interference distance. For simplicity, we assume that the mutually interfered region can be approximated as an annulus sector as shown in the figure. Suppose that all the users transmit at the same power and the interference distance is l_{RC}. Referring to Fig. 4, the central angle $\theta_{S,i}$ of a mutually interfered region in ring A_i is equal to

$$\theta_{S,i} = 2\sin^{-1}\left(\frac{l_{RC}}{r_i + r_{i-1}}\right) \quad \text{for } l_{RC} < (r_i + r_{i-1}). \quad (9)$$

If $l_{RC} \geqslant (r_i + r_{i-1})$, we define $\theta_{S,i} = 2\pi$. This means that the whole ring is in the same mutually interfered region. Clearly, the area of a mutually interfered region is $A_{S,i} = (\theta_{S,i}/2\pi)a_i$ and $a_i = \pi(r_i^2 - r_{i-1}^2)$ is the area of ring A_i.

Then, we define the *wireless collision domain* as the area in which at any instant at most one user can successfully deliver data traffic at a particular frequency. As shown in Fig. 4, the wireless collision domain in ring A_i is also approximated as an annulus sector with a central angle of $\theta_{W,i} = \theta_{S,i-1}$, and its area is $A_{W,i} = (\theta_{W,i}/2\pi)a_i$. The phenomenon of $\theta_{W,i} = \theta_{S,i-1}$ is due to the fact that the request-to-send/clear-to-send (RTS/CTS) mechanism is employed to avoid the hidden node problem. Referring to the example in Fig. 4, user A in ring A_i is sending data to user B in ring A_{i-1}. Meanwhile, since users P and A are not in the same mutually interfered region, user P in ring A_i can send an RTS request to users Q in ring A_{i-1}. However, user Q will not reply the CTS to P, because it has overheard the CTS of B and determined that the channel is busy. This example shows that users P and A are in the same wireless collision domain even though they are not in the same mutually interfered region. Furthermore, the central angle $\theta_{W,i}$ of wireless collision domain in ring A_i is determined by the

angle $\theta_{S,i-1}$ of mutually interfered region in the inner ring A_{i-1}, that is, $\theta_{W,i} = \theta_{S,i-1}$.

The example in Fig. 4 also shows that the transmission form the user in region V_R invalidates the RTS request of P. Hence, we define the region V_R with a central angle of $(\theta_{W,i} - \theta_{S,i})$ as the *working-in-vain region* of P. These effects of the ring structure on frame contentions will be incorporated into the throughput model later.

Note that the innermost ring A_1 is in the same wireless collision domain and $\theta_{W,1} = 2\pi$ since all users in ring A_1 can overhead the CTS from the gateway. By sectorizing ring A_1 as shown in Fig. 2, the number of contending users is decreased by a factor of three since $\theta_{W,1} = 2\pi/3$. Thus, the contention collisions can be also reduced to resolve the throughput bottleneck issue in the WMN.

4.3. Successful/unsuccessful transmission

As shown in Fig. 5, user P can successfully send data as long as no other user is transmitting in the adjacent wireless collision domains of P. Consider user P and its two wireless collision domains influenced by the closest two neighboring transmitters P_L and P_R, which are out of the mutually interfered regions of P as shown in the figure. Note that the considered area of angle $2\theta_{W,i}$ will be influenced by at most two neighboring transmitters (for example, users P_L and P_R). Other transmitters (for example, users P_L' and P_R') are too far away and will not affect the considered area. Let ψ_L and ψ_R represent the positions of P_L and P_R, respectively. If one of the transmitters P_L and P_R is within the working-in-vain regions of P, that is, $\psi_L, \psi_R \in [\theta_{S,i}, \theta_{W,i}]$, user P can still send the RTS request to user Q, but user Q cannot reply the CTS, as discussed in Section 4.2. Suppose that $Z_{W,i}$ is the average probability (average fraction of time) of a wireless collision domain in which a user is sending
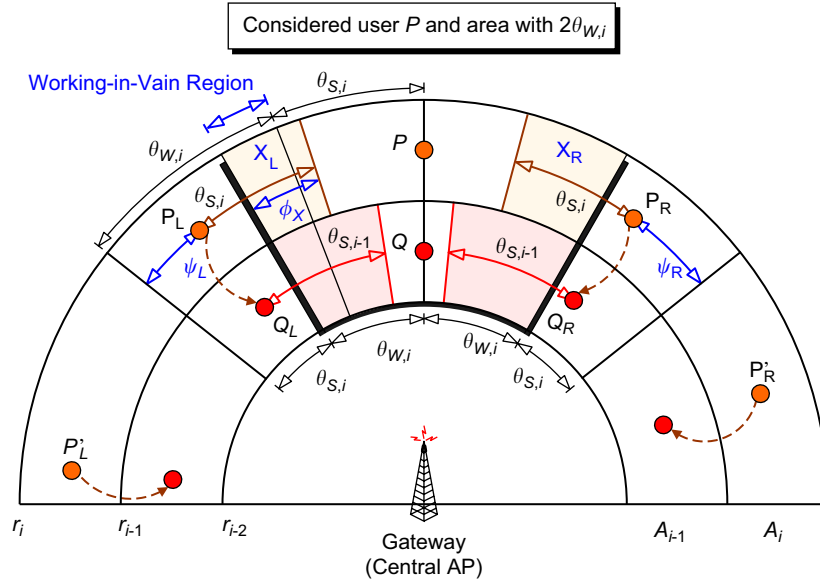
Fig. 5. The considered user P and two adjacent wireless collision domains, where user P is contending for the radio channel.

data as detailed in (30). Then, the working-in-vain probability p_v of user P can be expressed as

$$
\begin{aligned}
p_v &= 1 - \Pr\left\{\psi_L, \psi_R \notin [\theta_{S,i}, \theta_{W,i}]\right\} \\
&= 1 - \left[1 - Z_{W,i}\frac{\theta_{W,i} - \theta_{S,i}}{\theta_{W,i}}\right]^2,
\end{aligned}
\tag{10}
$$

where $Z_{W,i}$ accounts for the existence probability of transmitter P_L (P_R) which is affecting the considered area.

Now, we consider the case where both transmitters P_L and P_R are not in the working-in-vain regions of user P, that is, $\psi_L, \psi_R \in [0, \theta_{S,i}]$. In the considered area of angle $2\theta_{W,i}$, only the users in the area $\{2A_{W,i} - (X_L + X_R)\}$ can send RTS frames as shown in Fig. 5. Those users in regions X_L and X_R will not send their requests since they can sense the transmissions of P_L and P_R. Let $\overline{\phi}_X$ be the average central angle for region X_L, and $A_{W,i}$ be the area of a wireless collision domain of user P. Therefore, the average number of contending users $C_{1,i}$ in the considered area of angle $2\theta_{W,i}$ is equal to the average number of users in the area of $\{2A_{W,i} - (X_L + X_R)\}$. Consequently,

$$
\begin{aligned}
c_{1,i} &= \frac{\rho a_i}{2\pi}2(\theta_{W,i} - Z_{W,i}\overline{\phi}_X) \\
&= \frac{\rho a_i}{\pi}\left(\theta_{W,i} - \frac{Z_{W,i}}{\theta_{W,i}}\int_0^{\theta_{S,i}}\psi_L\,d\psi_L\right) \\
&= \rho(r_i^2 - r_{r-1}^2)\left(\theta_{W,i} - \frac{Z_{W,i}\theta_{S,i}^2}{2\theta_{W,i}}\right),
\end{aligned}
\tag{11}
$$

where ρ is the user density; $a_i = \pi(r_i^2 - r_{i-1}^2)$ is the area of ring A_i; $\theta_{S,i}$ is the central angle of the mutually interfered region

as defined in (9); $\phi_X = (\psi_L + \theta_{S,i}) - \theta_{S,i} = \psi_L$ is the central angle of region X_L and ψ_L is uniformly distributed in $[0, \theta_{W,i}]$ as shown in Fig. 5. Subject to the RTS/CTS procedures, the frame collisions may only occur when the contending users concurrently deliver their RTS requests. Let τ be the average probability of an active user sending the RTS request at the beginning of an activity slot. Suppose that π_0 is the average probability of a user being idle due to empty queue. Incorporating the impacts of ring structure on frame contention, the unsuccessful transmission probability p_u can be computed by

$$
p_u = p_v + (1 - p_v)[1 - (1 - \tau(1 - \pi_0))^{C_{1,i}-1}].
\tag{12}
$$

In (12), the first term is the probability that at least one transmitter is inside the working-in-vain regions of P. That is, user P will not receive the CTS response. The second term represents the probability that the RTS request from P is collided with other RTS frames.

Thus, given that the considered user has a non-empty queue, the probability that this user successfully/unsuccessfully sends data frame in an activity slot can be expressed as

$$
v_1 = \tau(1 - p_u),
\tag{13}
$$

$$
v_2 = \tau p_u.
\tag{14}
$$

4.4. Empty slot

As shown in Fig. 6, user P observes an empty slot if all the users in the adjacent mutually interfered regions of user P are silent. In the figure, the users in regions Y_L and Y_R will not send RTS since P_L and P_R are transmitting. Let $\overline{\phi}_Y$ be the average central angle of region Y_L, and $A_{S,i}$ be the area of a mutually interfered region of user P. The average number of contending
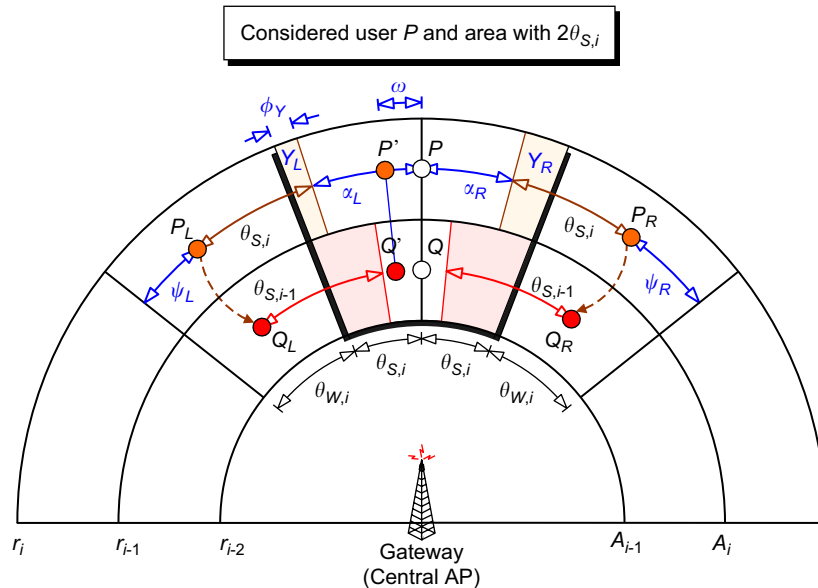
Fig. 6. The considered user P and its two mutually interfered regions, where user P is in backoff at the current slot.

users $C_{2,i}$ in the considered area of angel $2\theta_{S,i}$ is equal to the average number of users in the area of $\{2A_{S,i} - (Y_L + Y_R)\}$, and

$$c_{2,i} = \frac{\rho a_i}{2\pi} 2(\theta_{S,i} - Z_{W,i}\overline{\phi}_Y)$$

$$= \frac{\rho a_i}{\pi}\left(\theta_{S,i} - \frac{Z_{W,i}}{\theta_{W,i}}\int_0^{\theta_{W,i}}\max(0, \psi_L+\theta_{S,i}-\theta_{W,i})\,d\psi_L\right)$$

$$= \rho(r_i^2 - r_{r-1}^2)\left(\theta_{S,i} - \frac{Z_{W,i}\theta_{S,i}^2}{2\theta_{W,i}}\right), \tag{15}$$

where $\phi_Y = \max(0, \psi_L + \theta_{S,i} - \theta_{W,i})$ is the central angle of region Y_L. Therefore, from the viewpoint of the considered user, the empty-slot probability is

$$v_3 = (1 - \tau)[1 - \tau(1 - \pi_0)]^{c_{2,i}-1}, \tag{16}$$

where the first term is the probability of the considered user being in backoff, and the second term represents the probability that all the other users are in backoff or idle.

4.5. Successful/unsuccessful transmission from other users

To calculate the probability of successful transmission from other users, we consider user P and its adjacent mutually-interfered regions, as shown in Fig. 6. In the considered area of angle $2\theta_{S,i}$, the average number of contending users is $c_{2,i}$ as derived in (15). Given that user P is in backoff at the current slot, the probability that at least one user sends RTS is equal to $p_{\text{otr}} = 1 - [1 - \tau(1 - \pi_0)]^{c_{2,i}-1}$. Suppose that X_j is the probability of the considered area being influenced by j neighboring transmitters. In the considered area of angle $2\theta_{S,i}$, the conditional probability that there is at least one successful

transmission from other users is equal to

$$p_{\text{os}} = \frac{\sum_{j=0}^2 (2s_{1,j} - s_{2,j})X_j}{p_{\text{otr}}}, \tag{17}$$

where $X_j = \binom{2}{j} Z_{W,i}^j(1 - Z_{W,i})^{2-j}$, $s_{1,j}$ is the probability that there is a successful transmission in the left-side mutually interfered region of user P, and $s_{2,j}$ is the probability that there is a successful transmission in each mutually interfered region of P. Then, the probability that the considered user P observes successful/unsuccessful transmission(s) from other users in an activity slot can be expressed as

$$v_4 = (1 - \tau)p_{\text{otr}}p_{\text{os}}, \tag{18}$$

$$v_5 = (1 - \tau)p_{\text{otr}}(1 - p_{\text{os}}), \tag{19}$$

where the term $(1 - \tau)$ accounts for the probability of the considered user being in backoff. The successful probabilities $s_{1,j}$ and $s_{2,j}$ will be derived in Appendix A.

5. Throughput analysis

On top of the channel activity concept, we suggest an analytical throughput model for the ring-based WMN using the CSMA MAC protocol with RTS/CTS. In the throughput analysis, we also develop a bulk-arrival queueing model to describe user behavior under the non-saturation condition, considering the case where the forwarded frame and local frame may arrive at one user simultaneously. Although the 802.11a WLAN is used as an example here, the modeling framework can be applied to various wireless systems using different variation of CSMA protocol.

5.1. Background

Now we calculate the durations of a successful frame transmission and a collision in the IEEE 802.11a network. Let l be the payload size of data frame, m_a and m_c be the transmission PHY mode for data frame and that for control frame, respectively. Subject to the IEEE 802.11 CSMA MAC protocol with RTS/CTS, the successful frame transmission time T_S and collision time T_C are expressed as

$$\begin{aligned}
T_S = {}& T_{RTS}(m_c) + \delta + SIFS + T_{CTS}(m_c) + \delta + SIFS \\
& + T_{DATA}(l, m_a) + \delta + SIFS \\
& + T_{ACK}(m_c) + \delta + DIFS,
\end{aligned} \tag{20}$$

$$T_C = T_{RTS}(m_c) + \delta + EIFS, \tag{21}$$

where δ is the propagation delay; the durations of short interframe space (*SIFS*), distributed interframe space (*DIFS*) and extended interframe space ($EIFS = SIFS + T_{CTS}(m_c) + DIFS$) are specified in [14,15]. $T_{DATA}(l, m_a)$ is the transmission time for a data frame with payload size l using PHY mode m_a. $T_{RTS}(m_c)$, $T_{CTS}(m_c)$, and $T_{ACK}(m_c)$ are the transmission durations of RTS, CTS and acknowledgment (ACK) control frames using PHY mode m_c, respectively. According to the IEEE 802.11a WLAN standard [15], the values of $T_{DATA}(l, m_a)$, $T_{RTS}(m_c)$, $T_{CTS}(m_c)$ and $T_{ACK}(m_c)$ can be specified.

5.2. Carried traffic load of a mesh user

The carried traffic load of each mesh user includes its own traffic and the forwarded traffic from other users. Assume that an ideal load-balancing path selection is employed to avoid congested links [1,12]. Hence, all the users in the inner ring A_i evenly share the forwarded traffic from the outer ring A_{i+1}. Suppose that the users are uniformly distributed with the density ρ. The average number of users k_i in ring A_i is $k_i = \rho \pi (r_i^2 - r_{i-1}^2)$ and $(r_i - r_{i-1})$ is the width of ring A_i. Let R_D and $R_{F,i}$ be the average traffic load generated by one user and the forwarded traffic load per user in ring A_i, respectively. With the load-balancing path selection, the carried traffic load R_i of a mesh user in ring A_i can be expressed as

$$\begin{aligned}
R_i &= R_{F,i} + R_D = \frac{k_{i+1}}{k_i} R_{i+1} + R_D \\
&= \left[\frac{\sum_{j=i+1}^{n} k_j}{k_i} + 1 \right] R_D,
\end{aligned} \tag{22}$$

and the forwarded traffic load per user is $R_{F,i} = (\sum_{j=i+1}^{n} k_j/k_i) R_D$. For the outermost ring A_n, $R_i = R_D$ and $R_{F,i} = 0$.

5.3. MAC throughput

To evaluate the MAC throughput in the ring-based WMN, we should consider the impacts of the ring-based cell structure on frame contentions. Consider a binary exponential backoff procedure with the initial backoff window size of W. Let m_{bk} be the maximum backoff stage. The average backoff time can be calculated by

$$\begin{aligned}
\overline{B_k} ={}& (1 - p_u) \frac{W - 1}{2} + p_u(1 - p_u) \frac{2W - 1}{2} + \cdots \\
& + p_u{}^{m_{bk}}(1 - p_u) \frac{2^{m_{bk}} W - 1}{2} \\
& + p_u{}^{(m_{bk}+1)}(1 - p_u) \frac{2^{m_{bk}} W - 1}{2} + \cdots \\
={}& \frac{[1 - p_u - p_u(2p_u)^{m_{bk}}]W - (1 - 2p_u)}{2(1 - 2p_u)},
\end{aligned} \tag{23}$$

where p_u is the unsuccessful transmission probability with considering the effects of ring structure on frame contentions, as defined in (12). Since an active user sends RTS requests every $(\overline{B_k} + 1)$ slots on average [24], the transmission probability τ for an active user can be written as

$$\tau = \frac{1}{\overline{B_k} + 1} = \frac{2}{1 + W + p_u W \sum_{i=0}^{m_{bk}-1} (2p_u)^i}. \tag{24}$$

From (12) and (24), we can obtain the unique solution of τ and p_u for a given idle probability π_0 of a user. The idle probability π_0 will be derived by the following queueing model.

Fig. 7 illustrates the proposed bulk-arrival discrete-time queueing model for a mesh user, where the state variable s represents the number of frames queued at the user. Let l be the data frame payload size. In this WMN, the total traffic to a mesh user includes the forwarded traffic from other users with mean arrival rate $\lambda_F = R_{F,i}/l$ (frames/s) and the local traffic generated by user with mean rate $\lambda_L = R_L/l$. The forwarded frame and the local frame may arrive at one user simultaneously. According to the CSMA MAC protocol, in each activity time slot one user can successfully receive at most one forwarded frame. Therefore, we assume that the average arrival probability of forwarded traffic in an activity time slot is $\alpha_F = \lambda_F T_v$. Since the duration of activity slot is relatively short, we also assume that the probability of one local frame generated in a slot is $\alpha_L = \lambda_L T_v$. In addition, we note that a mesh user can successfully send one data frame in a slot with probability v_1, as discussed in Section 4.3.

Therefore, from above considerations, the number of frames queued at a user can be modeled by a semi-Markov model as shown in Fig. 7. The state-transition probabilities for the semi-Markov model can be expressed as

$$\begin{cases}
p_{s,s+2} = \chi_2 = \alpha_L \alpha_F (1 - v_1), \\
p_{s,s+1} = \chi_1 = \alpha_L \alpha_F v_1 + \alpha_L (1 - \alpha_F)(1 - v_1) \\
\qquad + (1 - \alpha_L) \alpha_F (1 - v_1), \\
p_{s,s-1} = \mu = (1 - \alpha_L)(1 - \alpha_F) v_1, \\
p_{s,s} = 1 - \chi_1 - \chi_2 - \mu,
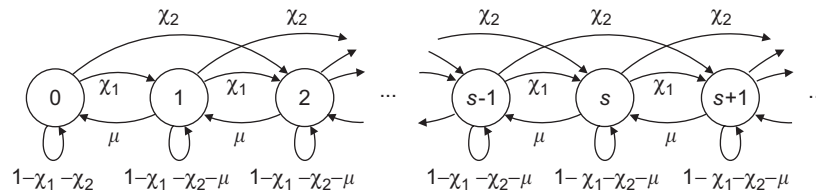\end{cases} \tag{25}$$

Fig. 7. State transition diagram for a user, where the state variable s is the number of frames queued at the user.

where $p_{s,s+2}$ represents the probability that two frames (one local frame and one forwarded frame) are simultaneously arrived in an activity slot, and no queued frame of the node is successfully delivered. Let π_s be the steady-state probability of s frames being queued at the node. Referring to Fig. 7, the global-balance equations for the considered queueing model can be written as

$$\begin{cases} 0 = -(\chi_1 + \chi_2 + \mu)\pi_s + \sum_{i=1}^{2} \chi_i \pi_{s-i} + \mu\pi_{s+1}, & s \geqslant 2, \\ 0 = -(\chi_1 + \chi_2 + \mu)\pi_1 + \chi_1\pi_0 + \mu\pi_2, \\ 0 = -(\chi_1 + \chi_2)\pi_0 + \mu\pi_1. \end{cases} \quad (26)$$

Then, by the probability generating function approach [8] with some manipulations, the generating function $\mathbb{P}(z)$ for the steady-state probability π_s can be expressed as

$$\mathbb{P}(z) = \sum_{s=0}^{\infty} \pi_s z^s = \frac{\mu\pi_0}{\mu - (\chi_1 + \chi_2)z - \chi_2 z^2}. \quad (27)$$

With the condition $\mathbb{P}(1) = \sum_{s=0}^{\infty} \pi_s = 1$, we can find the idle probability π_0 of a mesh user

$$\pi_0 = \frac{\mu - (\chi_1 + 2\chi_2)}{\mu} = 1 - \frac{\chi_1 + 2\chi_2}{\mu}. \quad (28)$$

Now we evaluate the MAC throughput of one user. With the activity slot concept, the average busy probability (average fraction of time) $Z_{O,i}$ of one user being sending data and the channel utilization $Z_{W,i}$ of a wireless collision domain can be expressed as

$$Z_{O,i} = \frac{v_1 T_1}{\sum_{j=1}^{5} v_j T_j}(1 - \pi_0) = \frac{v_1 T_1}{T_v}(1 - \pi_0), \quad (29)$$

$$Z_{W,i} = \rho A_{W,i} Z_{O,i}, \quad (30)$$

where v_1 is the probability that one user successfully sends a frame in an activity slot, $T_1 = T_S$ is the time duration for successful frame transmission, T_v is the average duration of an activity slot, and $\rho A_{W,i}$ is the number of users in a wireless collision domain. From (8), (13) and (28)–(30), v_1, T_v and π_0 can be calculated by an iterative method. Then, the capacity $H_i(d)$ of a mesh link between two users at a separation distance d can be calculated by

$$H_i(d) = \frac{v_1 T_1}{T_v} \cdot \frac{l}{T_S} = \frac{v_1 l}{T_v}, \quad (31)$$

where l is the payload size of data frame. It is noteworthy that the payload size l of data frame is affected by the separation distance d and the PHY mode m_a, which will be discussed in the following.

5.4. Impact of hop distance on transmission rate

In a multi-hop network, the hop distance will also affect the throughput of relay link. Generally, the radio signal is affected by path loss, shadowing as well as multi-path fading. With all these radio channel effects, we assume that for a given transmission power the average reception ranges for eight PHY modes are d_j, $j = 1, 2, \ldots, 8$, where $d_1 > d_2 > \cdots > d_8$. In principle, two users with a shorter separation distance can transmit at a higher data rate. Therefore, the transmission PHY mode m_a is determined according to the separation distance d between two users. That is,

$$m_a = j \quad \text{if } d_{j+1} < d \leqslant d_j. \quad (32)$$

Furthermore, we suggest that all data frames have the same transmission time $T_{\text{DATA}}(l, m_a)$. That is, the payload size l of data frame is determined by the adopted PHY mode m_a. As in [4,10], the same transmission time for each data frame can achieve fairness and avoid throughput degradation due to low-rate transmissions.

6. Numerical results

In this section, we investigate the tradeoff between user throughput and cell coverage for the ring-based WMN. The analytical results are obtained by means of the proposed analytical throughput model and the optimization approach. The system parameters are summarized in Table 1. In this paper, the 802.11a WLAN is used as an example. The transmission PHY mode m_a for data frame is determined by the hop distance. Besides, the control frames (RTS/CTS/Acknowledge frames) are transmitted with PHY mode $m_c = 1$ for reliability. The user density is assumed to be $\rho = 10^{-4}$ (users/m^2). We assume that each user transmits at the same power and the interference range is $l_{RC} = \gamma_I d_{\max}$, where γ_I is 1.3. By using the ring-based frequency planning scheme as in Section 2.2, four buffer rings can be achieved to avoid inter-ring co-channel interference. As in [4], the chosen data frame payload sizes for eight PHY modes are {425, 653, 881, 1337, 1793, 2705, 3617, 4067} (bytes). Referring to the measured results in [5], at a given transmission power the corresponding average reception ranges are

Table 1
System parameters for numerical examples

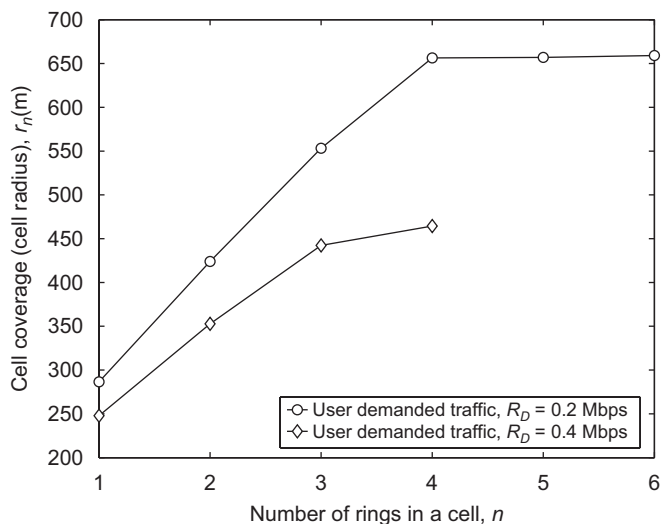| Symbol	Item	Nominal value
ρ	User density	$(100)^{-2}$ (users/m^2)
R_D	Demanded traffic of each user	0.4, 0.8 Mb/s
d_{min}	Min. ring width, i.e., $(1/\sqrt{\rho})$	100 m
d_{max}	Max. reception range	300 m
l_{RC}	Interference range ($\gamma_I D_{max}$)	$1.3 * d_{max}$ (m)
m_a	PHY mode for data frame	1–8 (6–54 Mb/s)
m_c	PHY mode for control frame	1 (fixed at 6 Mb/s)

Fig. 8. Cell coverage (cell radius r_n) versus the number of rings n in a cell, for various user demanded traffic R_D.

$d_j = \{300, 263, 224, 183, 146, 107, 68, 30\}$ (m). These reception ranges may vary for different environments. However, the proposed optimization approach is general enough for different WMNs with various reception ranges.

6.1. Tradeoff between user throughput and cell coverage

Fig. 8 illustrates cell coverage (defined as cell radius r_n) against the number of rings n in a mesh cell for various demanded traffic per user R_D. The optimal ring widths are determined by the proposed optimization approach. In general, as the number of rings n in a cell increases, cell coverage also increases. However, because of the limit of link capacity of users in the innermost ring near the gateway, cell coverage remains the same for a larger n (see $n \geqslant 4$ in the case with $R_D = 0.2$ Mb/s). Besides, it is shown that the number of rings n in a cell has a maximum value. For accommodating the increasing traffic as n increases, the ring width will be shortened to reduce the number of contending users and improve the link capacity. For example, if $n = 3$, the optimal ring widths for $R_D = 0.4$ Mb/s are $\{113, 119, 211\}$ (m). As the number of rings increases to $n = 4$, the optimal ring widths are reduced to $\{100, 103, 126, 136\}$ (m). However, since the minimum
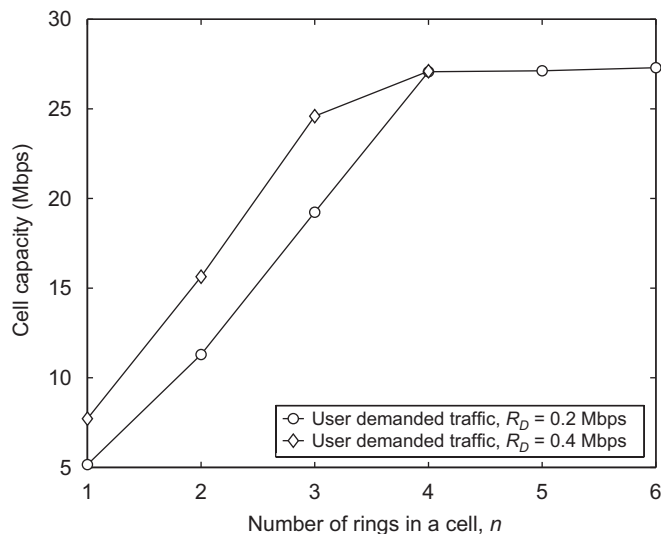

Fig. 9. Cell capacity versus the number of rings n in a cell, for various user demanded traffic R_D.

allowable ring width is constrained by the node density as in (3), no feasible solution can be found for a larger n and thus the maximum value of n exists. In this example, the maximum number of rings in a cell is $n = 6$ for $R_D = 0.2$ and $n = 4$ for $R_D = 0.4$ Mb/s.

From Fig. 8, we can observe the tradeoff between user throughput and cell coverage. To guarantee the throughput for each user, the number of users in a cell and cell coverage should be properly decreased when the user demanded traffic R_D increases. In this example, when the user demanded traffic R_D increases from 0.2 to 0.4 Mb/s, the optimal cell coverage is reduced from 659 (m) at $n = 6$ to 465 (m) at $n = 4$. The corresponding optimal ring widths are $\{100, 100, 100, 100, 109, 150\}$ (m) for $R_D = 0.2$ and $\{100, 103, 126, 136\}$ (m) for $R_D = 0.4$ Mb/s, respectively.

In Fig. 9, cell capacity (defined as the overall throughput of a cell, $\rho \pi r_n^2 R_D$) against the number of rings n in a cell for various user demanded traffic R_D is shown. Because each user generates more traffic, a larger R_D can achieve higher cell capacity for $n \leqslant 3$, although with a smaller cell coverage. However, constrained by the link capacity of users in the innermost ring, the optimal cell capacity for various user demanded traffic R_D are almost the same at about 27 Mb/s as shown in the figure.

In the above figures, we investigate the interaction between user throughput and cell coverage. The optimal solution is determined by the proposed optimization approach, subject to the constraints on the link capacity and the ring width. These figures show that by ring-based frequency planning and properly designing the ring widths, the optimal cell capacity and coverage can be simultaneously achieved with a guaranteed throughput for each user.

6.2. Impact of ring sectorization

Fig. 10 compares the impact of ring sectorization on cell coverage, for $R_D = 0.4$ Mb/s. As shown in the figure, since
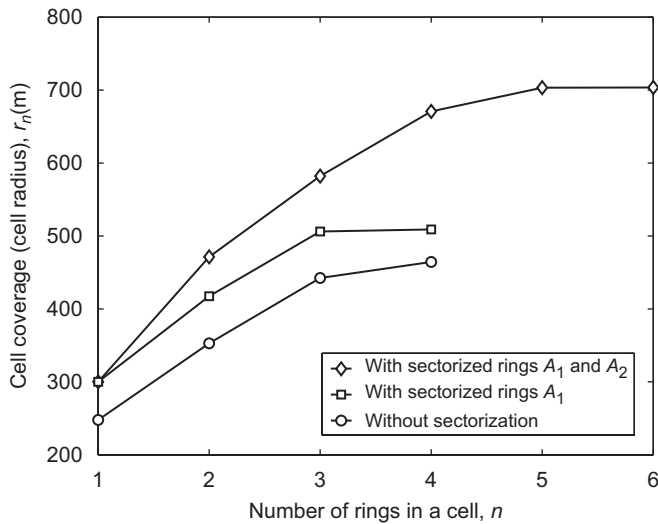
Fig. 10. Effect of ring sectorization on cell coverage (cell radius r_n), for the user demanded traffic $R_D = 0.4$ Mb/s.
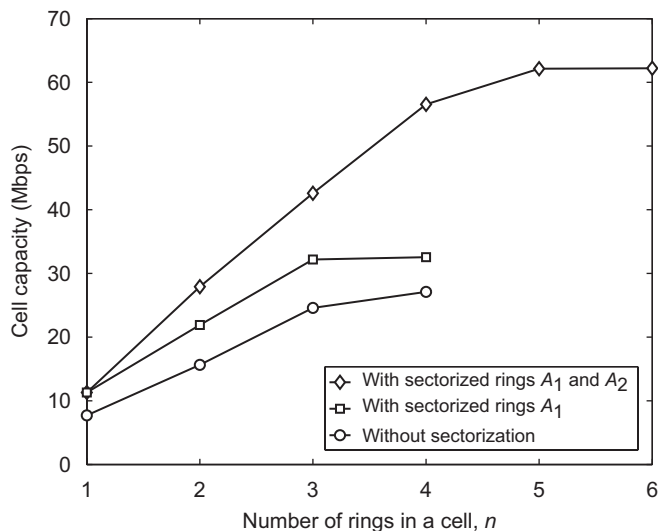

Fig. 11. Effect of ring sectorization on cell capacity, for the user demanded traffic $R_D = 0.4$ Mb/s.

sectorizing the inner rings can reduce the number of contending users to overcome the throughput bottleneck issue near the gateway, cell coverage can be extended to serve more users. One can observe from the figure that if only ring A_1 is sectorized, the optimal cell coverage can increase from 464 to 508 (m) at $n = 4$. If sectorizing both rings A_1 and A_2, the optimal cell coverage increases to 703 (m) at $n = 6$.

In Fig. 11, the effect of ring sectorization on cell capacity for $R_D = 0.4$ Mb/s is shown. In the figure, by sectorizing ring A_1, the optimal cell capacity can be improved by 20% over the case without sectorization. If the congested inner rings A_1 and A_2 are sectorized, the throughput bottleneck issue near the gateway can be overcome. By doing so, the optimal cell capacity will be further improved by 90% over the case with only sectorizing ring A_1.

Clearly, sectoring more inner rings can improve cell coverage and capacity. For sectorizing more rings, however, the system requires more available non-overlapping channels [16,23], since each mesh cell should be allocated with more channels to ensure sufficient buffer rings and reuse distance.

7. Conclusions

This paper has investigated the tradeoff between user throughput and cell coverage in the WMN. To overcome the scalability and throughput bottleneck issues in the WMN, a scalable multi-channel ring-based WMN has been employed. An optimization approach has been applied to maximize coverage and capacity for the considered WMN, subject to the user throughput requirement.

In the ring-based WMN, a simple ring-based frequency planning scheme has been employed to reduce collisions, and to make the network more scalable in terms of coverage. We have also suggested sectorizing the congested inner rings to resolve the throughput bottleneck issue of the WMN. From the system design perspective, this paper has three important components. First, an analytical throughput model has been developed, which considers the effects of ring-based cell structure and frame contentions in the CSMA MAC protocol. Second, we have developed a bulk-arrival semi-Markov queueing model to describe user behavior in the non-saturation condition. Third, to investigate the optimal tradeoff between user throughput and cell coverage, we have applied an optimization approach to determine the optimal number of rings and the associated ring widths in a mesh cell. Numerical results have demonstrated that the optimal system parameters (that is, the number of rings and ring widths) can be determined analytically. In addition, both the capacity enhancement and coverage extension can be achieved with a guaranteed throughput for each user.

Appendix A. Successful probabilities, $s_{1,j}$ and $s_{2,j}$

Now we derive the probabilities $s_{1,j}$ and $s_{2,j}$ mentioned in Section 4.5. As shown in Fig. 6, suppose that the considered area of angle $2\theta_{S,i}$ is influenced by two neighboring transmitters P_L and P_R. Let ω represent the position of the contending user P', ψ_L and ψ_R be the positions of the neighboring transmitters P_L and P_R. Accordingly, the central angles for regions $\{A_{S,i} - Y_L\}$ and $\{A_{S,i} - Y_R\}$ can be written as $\alpha_L = \theta_{S,i} - \max(0, \psi_L + \theta_{S,i} - \theta_{W,i})$ and $\alpha_R = \theta_{S,i} - \max(0, \psi_R + \theta_{S,i} - \theta_{W,i})$, respectively. Suppose that $\tau_e = \tau(1 - P_0)$ is the effective transmission probability for one user.

Then, given the positions ω, ψ_L and ψ_R, the conditional probability that there is a successful transmission in the left-side mutually interfered region of user P can be expressed as

$$s_{1,j}(\psi_L, \psi_R, \omega)$$
$$= \begin{cases} \binom{\frac{\rho a_i}{2\pi}\alpha_L - 1}{1} \tau_e(1-\tau_e)^{\frac{\rho a_i}{2\pi}(\beta_L+\beta'_L)-2} \\ \quad \text{for } \max(0, \psi_R - \theta_{S,i}) \leqslant \omega \leqslant \max(0, \theta_{S,i} - \psi_L), \\ 0 \text{ otherwise.} \end{cases} \quad (33)$$

In (33), the term $\left(\begin{smallmatrix}(\rho a_i/2\pi)\alpha_L-1\\1\end{smallmatrix}\right)$ represents the probability that only user P' sends an RTS request in the left-side mutually interfered region of user P. The term $(1-\tau_e)^{(\rho a_i/2\pi)(\beta_L+\beta'_L)-2}$ accounts for the probability that all the users except for P and P' in the adjacent wireless collision domains of P' are in backoff or idle, where $\beta_L = \min(\omega + \theta_{W,i}, (\theta_{S,i} + \theta_{W,i}) - (\psi_L + \theta_{S,i})) = \min(\omega + \theta_{W,i}, \theta_{W,i} - \psi_L)$ and in the same way $\beta'_L = \min(\theta_{W,i} - \omega, \theta_{W,i} - \psi_R)$. In addition, the constraint for ω means that both the neighboring transmitters P_L and P_R are not inside the working-in-vain regions of P'.

By the same method, the conditional probability that there is a successful transmission in each mutually interfered region of user P can be obtained from

$$s_{2,j}(\psi_L, \psi_R, \omega) = s_{1,j}(\psi_L, \psi_R, \omega)$$
$$\times \left[\left(\begin{matrix}\frac{\rho a_i}{2\pi}\beta_R\\1\end{matrix}\right)\tau_e(1-\tau_e)^{\frac{\rho a_i}{2\pi}\beta'_R-1}\right]. \qquad (34)$$

Here, the term within brackets represents the probability that there is also a successful transmission in the right-side mutually interfered region of user P, where $\beta_R = \max(0, (\theta_{S,i} + \theta_{W,i}) - (\psi_R + \theta_{S,i-1}) - (\theta_{W,i} - \omega)) = \max(0, (\theta_{S,i} - \psi_R) - (\theta_{W,i} - \omega))$ and $\beta'_R = \max(0, (\theta_{S,i} + \theta_{W,i}) - (\psi_R + \theta_{S,i}) - (\theta_{W,i} - \omega)) = \max(0, \omega - \psi_R)$.

By averaging over the positions ω, ψ_L and ψ_R, the probabilities $s_{1,j}$ and $s_{2,j}$ for $j = 2$ can be computed by

$$s_{t,j} = \frac{1}{\theta_{W,i}^2} \int_0^{\theta_{W,i}} \int_0^{\theta_{W,i}} \int_0^{\alpha_L} \frac{s_{t,j}(\psi_L, \psi_R, \omega)}{\alpha_L} \, d\omega \, d\psi_R \, d\psi_L,$$
$$\text{for } t = 1, 2. \qquad (35)$$

In this section, we take the case of $j = 2$ as an example to explain how to evaluate the successful probability $s_{t,j}$. By the same reasoning, one can also calculate the probabilities $s_{t,j}$ for $j = 0, 1$. Thus, the detailed derivations are omitted here.

References

[1] I.F. Akyildiz, X. Wang, W. Wang, Wireless mesh networks: a survey, Comput. Networks 47 (4) (2005) 445–487.

[2] G. Bianchi, Performance analysis of the IEEE 802.11 distributed coordination function, IEEE J. Select. Areas Commun 18 (3) (2000) 535–547.

[3] P. Chatzimisios, A.C. Boucouvalas, V. Vitsas, Packet delay analysis of the IEEE MAC 802.11 protocol, IEE Electron. Lett. 39 (2003) 1358–1359.

[4] L.J. Cimini, Z. Kostic, K.K. Leung, H. Yin, Packet shaping for mixed rate 802.11 wireless networks, United States Patent Application Number: US 20030133427, July 2003.

[5] CISCO, Data Sheet: Cisco Aironet 1200 Series Access Point. Available from: ⟨http://www.cisco.com/⟩.

[6] X.J. Dong, P. Variya, Saturation throughput analysis of IEEE 802.11 wireless LANs for a lossy channel, IEEE Commun. Lett. 9 (2) (2005) 100–102.

[7] T. Fowler, Mesh networks for broadband access, IEE Rev. 47 (1) (2001) 17–22.

[8] D. Gross, C.M. Harris, Fundamentals of Queueing Theory, third ed., Wiley, New York, 1998.

[9] P. Gupta, R. Kumar, The capacity of wireless networks, IEEE Trans. Inform. Theory 46 (2000) 388–404.

[10] M. Heusse, F. Rousseau, G. Berger-Sabbatel, A. Duda, Performance anomaly of 802.11b, in: Proceedings of IEEE INFOCOM'03, April 2001, pp. 986–995.

[11] G. Holland, N.H. Vaidya, Analysis of TCP performance over mobile ad hoc networks, Wireless Networks 8 (2–3) (2002) 275–288.

[12] P. Hsiao, A. Hwang, H. Kung, D. Vlah, Load-balancing routing for wireless access networks, in: Proceedings of IEEE INFOCOM'01, March 2003.

[13] J.-H. Huang, L.-C. Wang, C.-J. Chang, Capacity and QoS for a scalable ring-based wireless mesh network, IEEE J. Select. Areas Commun. 24 (11) (2006) 2070–2080.

[14] IEEE 802.11, Wireless LAN Medium Access Control (MAC) and Physical Layer (PHY) Specifications, Standard, IEEE, August 1998.

[15] IEEE 802.11a, Part 11: Wireless LAN, Medium Access Control (MAC) and Physical Layer (PHY) Specifications: High-Speed Physical Layer in the 5 GHz Band, supplement to IEEE 802.11 Standard, September 1999.

[16] ITU World Radiocommunication Conference 2003, Resolution 229 [COM5/16], Use of the bands 5150–5250 MHz, 5250–5350 MHz and 5470–5725 MHz by the mobile service for the implementation of wireless access systems including radio local area networks, July 2003.

[17] K. Jain, J. Padhye, V.N. Padmanabhan, L. Qiu, Impact of interference on multi-hop wireless network performance, in: Proceedings of ACM MobiCom'03, September 2003.

[18] J. Jun, M. Sichitiu, The nominal capacity of wireless mesh networks, IEEE Wireless Commun. Mag. 10 (5) (2003) 8–14.

[19] J. Li, C. Blake, D.S.J. De Couto, H.I. Lee, R. Morris, Capacity of ad hoc wireless networks, in: Proceedings of ACM MobiCom'01, July 2001.

[20] S. Naghian, J. Tervonen, Semi-infrastructure mobile ad-hoc mesh networking, in: Proceedings of IEEE PIMRC'03, September 2003, pp. 1069–1073.

[21] R. Pabst, et al., Relay-based deployment concepts for wireless and mobile broadband radio, IEEE Commun. Mag. 42 (9) (2004) 80–89.

[22] L. Qiu, P. Bahl, A. Rao, L. Zhou, Troubleshooting multihop wireless networks, microsoft research, Technical Report MSR-TR-2004-11, November 2004.

[23] Wi-Fi Alliance, Wi-Fi Alliance Certification of IEEE 802.11g, Q&A. Available from: ⟨http://www.wi-fi.org/opensection/pdf/tgg_qa.pdf⟩.

[24] Y.C. Yay, K.C. Chua, A capacity analysis for the IEEE 802.11 MAC protocol, Wireless Network (2001) 159–171.

[25] M. Zhang, R. Wolff, Crossing the digital divide: cost-effective broadband wireless access for rural and remote areas, IEEE Commun. Mag. 42 (2) (2004) 99–105.

Jane-Hwa Huang received the B.S., M.S., and Ph.D. degrees in electrical engineering from the National Cheng-Kung University, Taiwan, ROC, in 1994, 1996, and 2003, respectively.

He joined the Department of Communication Engineering, National Chiao-Tung University, Taiwan, as a Postdoctoral Researcher from 2004 to January 2006, and a Research Assistant Professor since January 2006. His current research interests are in the areas of wireless networks, wireless multi-hop communications, vehicular communication networks, and radio resource management.

Li-Chun Wang received the B.S. degree in electrical engineering from the National Chiao-Tung University, Hsinchu, Taiwan, ROC, in 1986, the M.S. degree in electrical engineering from the National Taiwan University, Taipei, Taiwan, in 1988, and the M.Sc. and Ph.D. degrees in electrical engineering from Georgia Institute of Technology, Atlanta, in 1995 and 1996, respectively.

From 1990 to 1992, he was with Chunghwa Telecom. In 1995, he was affiliated with Northern Telecom in Richardson, Texas. From 1996 to 2000, he was with AT&T Laboratories, where he was a Senior Technical Staff Member in the Wireless Communications Research Department. Since August 2000, he has joined the Department of Communication Engineering of National Chiao-Tung University in Taiwan as an Associate Professor and has been promoted to a full professor since August 2005. Dr. Wang was a corecipient of the Jack Neubauer Best Paper Award from the IEEE Vehicular Technology Society in 1997. His current research interests are in the areas of cellular architectures, radio network resource management, cross-layer optimization for cooperative and cognitive wireless networks. He is the holder of three US patents with three more pending.

Chung-Ju Chang was born in Taiwan, ROC, in August 1950. He received the B.E. and M.E. degrees in electronics engineering from National Chiao-Tung University (NCTU), Hsinchu, Taiwan, in 1972 and 1976, respectively, and the Ph.D. degree in electrical engineering from National Taiwan University (NTU), Taiwan in 1985.

From 1976 to 1988, he was with Telecommunication Laboratories, Directorate General of Telecommunications, Ministry of Communications, Taiwan, as a Design Engineer, Supervisor, Project Manager, and then Division Director. In the meantime, he also acted as a Science and Technical Advisor for the Minister of the Ministry of Communications from 1987 to 1989. In 1988, he joined the Faculty of the Department of Communication Engineering, College of Electrical Engineering and Computer Science, National Chiao-Tung University as an Associate Professor. He has been a Professor since 1993. He was Director of the Institute of Communication Engineering from August 1993 to July 1995, Chairman of Department of Communication Engineering from August 1999 to July 2001, and the Dean of the Research and Development Office from August 2002 to July 2004. Also, he was an Advisor for the Ministry of Education to promote the education of communication science and technologies for colleges and universities in Taiwan during 1995–1999; he is acting as a Committee Member of the Telecommunication Deliberate Body, Taiwan. He serves as Editor for IEEE Communications Magazine and Associate Editor for IEEE Transactions on Vehicular Techonology. His research interests include performance evaluation, wireless communication networks, and broadband networks. Dr. Chang is a member of the Chinese Institute of Engineers (CIE) and an IEEE Fellow.